Potential energy surfaces for the $^3A''$ and $^3A'$ electronic states of the O(^3P) + HCl system

B. Ramachandran[a]

Chemistry, College of Engineering & Science,

Louisiana Tech University

Ruston, LA 71272

Kirk A. Peterson[b]

Department of Chemistry,

Washington State University

Pullman, WA, 99164-4630

[a] E-mail: ramu@latech.edu

[b] E-mail: kipeters@wsu.edu

ABSTRACT

We report *ab initio* calculations at the MRCI+Q/CBS level of theory for the $^3A''$ and $^3A'$ electronic states of the O(^3P) + HCl system, where the complete basis set (CBS) energies are obtained by extrapolating MRCI+Q/aug-cc-pV*n*Z (*n* = 2, 3, 4) energies. Potential energy surfaces for these electronic states are generated by interpolating these energies using the Reproducing Kernel Hilbert Space (RKHS) method. The reaction barrier on the interpolated $^3A''$ surface at the MRCI+Q/CBS level of theory is 11.86 kcal/mol. The potential energy surface was then scaled to yield a barrier height close to that predicted by CCSD(T) and MRCI+Q benchmark calculations, namely, 10.60 kcal/mol. The fact that the $^3A''$ and $^3A'$ electronic states are degenerate at collinear and asymptotic regions of configuration space was used to scale the collinear reaction barrier on the $^3A'$ surface from the MRCI+Q/CBS value of 15.15 kcal/mol to match that of the scaled $^3A''$ surface, 13.77 kcal/mol. The potential energy surfaces thus obtained appear to be the most accurate to date for the reaction O(^3P) + HCl $\rightarrow$ OH + Cl. The potential energy surface for the $^3A''$ state contains a fairly deep van der Waals well on the product side of the reaction barrier at a rather sharp O-H-Cl angle (67°) and a shallow well on the reactant side at collinear O-H-Cl geometry. Details of the *ab initio* calculations, the fitting procedure, and characterization of the saddle and stationary points are presented.

31.15.Ar, 31.25.-v, 31.25.Nj, 31.25.Qm, 34.20.Gj, 34.20.Mq

I. Introduction

The subject of this paper is the construction of accurate potential energy surfaces (PES's) for studying the dynamics of the reaction $O(^3P) + HCl \rightarrow OH + Cl$. This reaction proceeds primarily by the $^3A''$ electronic state at low temperatures, but the role of the $^3A'$ state –which has a higher reaction barrier– becomes increasingly significant as the temperature rises. Potential energy surfaces currently available for the $^3A''$ electronic state of this system have all been shown to be lacking in one respect or the other (see below). The $^3A''$ PES reported here is based on more extensive *ab initio* calculations than the earlier versions and we believe that it addresses the shortcomings of the earlier surfaces. This paper also reports the first PES based on *ab initio* calculations for the $^3A'$ electronic state for the $O(^3P) + HCl \rightarrow OH + Cl$ reaction.

Theoretical investigations of the $O(^3P) + HCl$ reaction prior to the nineties were carried out on model PES's constructed under the assumption that the reaction barrier corresponded to a collinear O-H-Cl geometry.[1 2 3 4 5] In 1989, the *ab initio* investigations of Gordon *et al.*,[6] established that the minimum energy saddle point, which lies on the lowest energy $^3A''$ state, corresponds to a bent O-H-Cl geometry. The importance of a proper treatment of electron correlation effects for obtaining the reaction barrier for this system became clear from their work. Depending on the theoretical method and basis set used, the calculated barrier height ranged from 27.2 to 11.9 kcal/mol. High levels of theory [CCSD(T)] and large one electron basis sets [MC-311G(2*d*, 2*p*)] were necessary to get the lower barriers.

As a continuation of this work, Koizumi, Schatz, and Gordon (KSG) constructed the first realistic PES for the $^3A''$ state, based on MP2/6-31G(*d*,*p*) energies.[7] KSG found that in order to

obtain good agreement between quantum mechanical and experimental rate coefficients at 293 K, the MP2/6-31G(*d,p*) energies had to be "shifted" so as to reduce the barrier height from 18.8 to 8.5 kcal/mol. However, this barrier was found to be too low (i.e., the predicted thermal rate constants too high) by later, more extensive quantum mechanical calculations.[8 9 10 11 12] A new representation of the $^3A''$ electronic state, called the S4 surface, based on SEC-scaled[13] MRCI+Q/cc-pVTZ energies, was reported by Ramachandran *et al*. in 1999.[14] The S4 surface has a barrier height of 9.78 kcal/mol. The *ab initio* energies calculated for this purpose revealed, for the first time, the existence of a deep van der Waals minimum in the product channel of this reaction. Quasiclassical trajectory calculations on the S4 surface were able to reproduce, near-quantitatively, the state-to-state integral cross sections, the OH rotational distributions, the OH $v'=1/v'=0$ branching ratios,[14] and energy disposal patterns[15] observed in the experiments of the Zare group.[16] Variational Transition State Theory (VTST)[17] calculations of the thermal rate coefficients on this surface also led to excellent agreement with experimental values over a broad temperature range.[18] In these respects, the S4 PES can be said to be more accurate than the KSG surface. However, more recently, quantum mechanical calculations of the thermal rate coefficients by Skokov *et al.*,[18 19] and Nobusada *et al.*,[20] have revealed that the reaction barrier on the S4 surface may be too low, and perhaps too narrow in the sense of permitting too much tunneling.

This paper represents a new attempt to calculate an accurate PES for the $^3A''$ state of the O(^3P) + HCl system and the first reported attempt at obtaining a PES for the $^3A'$ state. The *ab initio* calculations for the present work were carried out at the multireference configuration interaction (MRCI) level of theory with the addition of the multireference Davidson correction for higher excitations (MRCI+Q). These calculations used successively larger members from the

aug-cc-pV*n*Z (AV*n*Z) family of basis sets of Dunning and co-workers,[21] where n = 2, 3, and 4. The basis sets for O and Cl were slightly modified as described in Section II. The MRCI+Q/AV*n*Z energies were then extrapolated to the complete basis set (CBS) limit using an expression[22] used by one of the authors with considerable success in the past.[23,24] For the $^3A''$ state, additional *ab initio* calculations were performed at the MRCI, CCSD(T), and CCSDT levels of theory to get reliable estimates of the barrier height for this reaction. The PES's presented below are based on fits to MRCI+Q/CBS energies. These PES's (but not the MRCI+Q/CBS energies) are then scaled to closely reproduce the best estimates of reaction barrier heights, which were essentially identical to the CCSD(T)/CBS results. Quantum thermal rate constants calculated using these surfaces (the following paper[25]) compare very favorably with available experimental data, which span the temperature range 293-3197 K.[26]

The remainder of this paper is organized as follows. In Section II, we discuss the details of the *ab initio* calculations including basis set modifications and the extrapolation to the complete basis set (CBS) limit. Section III deals with the details of the benchmark calculations to establish the barrier height on the $^3A''$ surface and to determine the locations and the properties of the van der Waals minima. Section IV describes the procedures used to obtain a smooth fit through the MRCI+Q/CBS energies to generate the two surfaces and the scaling of the MRCI+Q/CBS three body term to reproduce the CCSD(T) barrier height on the $^3A''$ surface. Section V is a discussion of the properties of the two potential surfaces, with special attention given to characterizing the saddle points and the stationary points on the $^3A''$ surface. Section VI presents a summary of this work.

II. Details of the *Ab Initio* Calculations

The basis sets and correlation methods used to develop the PES's of this work closely parallel those used by one of the authors for the singlet ground state surface of HOCl.[27] In order to account for errors due to an incomplete 1-particle basis set, three basis sets ranging in size from double to quadruple-zeta were used at each point calculated on the PES. These sets were constructed from the standard correlation consistent basis sets (cc-pV*n*Z with *n*=D,T,Q, etc.) of Dunning and co-workers[28] with the addition of a single set of diffuse *s, p,* and *d* functions on O and Cl and diffuse *s* and *p* functions on H. The latter functions were taken from the standard aug-cc-pV*n*Z sets,[29] yielding sets denoted by AV*n*Z′ (*n* = D, T, Q). It should be noted that AVDZ′ is equivalent to the standard aug-cc-pVDZ set. In addition, it is now well-known that accurate calculations on Cl-containing molecules require the addition of a tight, i.e., high exponent, *d* function to the cc-pV*n*Z basis sets. [30] While new cc-pV(*n*+*d*)Z basis sets are now available for this purpose,[30] we have elected to use the same tight *d* exponents used previously for HOCl (namely 1.689 for DZ, 5.156 for TZ, and 6.654 for QZ). The total energies calculated on the PES with each of these 3 basis sets (AVDZ+*d*, AVTZ′+*d*, and AVQZ′+*d*) were then extrapolated to the approximate complete basis set (CBS) limit via[22]

$$E(n) = E_{\mathrm{CBS}} + Be^{-(n-1)} + Ce^{-(n-1)^2}. \qquad (1)$$

Electron correlation was treated using the internally contracted multireference CI method[31] with the multireference Davidson correction[32] (MRCI+Q) using a full valence complete active space[33] (CAS) reference function (14 electrons in 9 orbitals, i.e., 322 configuration state functions for the ^{3}A″ state). Separate MRCI+Q calculations for both the $1^3A''$ and $1^3A'$ states were carried out. Unless otherwise noted, only the valence electrons were correlated. The orbitals used in these MRCI calculations were taken from state-averaged CASSCF calculations

with the same full valence active space. In each case the core orbitals were obtained from Hartree-Fock calculations on the closed shell $HOCl^{2-}$ species, and the O 2*s* and Cl 3*s* orbitals were constrained to be doubly occupied. This latter restriction was lifted in the MRCI reference function. A total of 6 triplet states were averaged in the CASSCF procedure, which corresponded to the 3 states of A' and 3 states of A'' symmetry (all calculations were carried out in the C_s point group) that can be formed from the $Cl(^2P)$ + $OH(^2\Pi)$ products. In the case of the $O(^3P)$ + $HCl(^1\Sigma^+)$ reactants, however, only 1 state of A' and 2 states of A'' symmetry correlate to this asymptote. Thus, in order to smoothly connect the orbitals between reactants and products and obtain orbitals reflecting the correct degeneracy in both cases, geometry-dependent weights were used in the CASSCF calculations. Correct behavior was obtained by first assigning a (unnormalized) weight of 1.0 for each of the first A' and A'' states. Weights for the second and third A' states, as well as for the second A'' state were given by the greater of zero and the weight $w_2 = 1 - e^{-(r_{HCl}-r^0_{HCl})}$, where $r^0_{HCl} = 2.41a_0$. The weight for the third A'' state was then obtained as the greater of the value of w_2 and $w_1 = 1 - e^{-(r_{OH}-r^0_{OH})}$, where $r^0_{OH} = 1.83a_0$.

In addition to the MRCI+Q calculations described above, coupled cluster (CC) calculations, namely singles and doubles coupled cluster with perturbative triples [CCSD(T)],[34] were also carried out for the reactants, products, and transition state on the $^3A''$ surface. These calculations generally used restricted open-shell HF (ROHF) orbitals within the frozen core approximation using the R/UCCSD(T) variant of open-shell CC theory.[35 36] In this method small amounts of spin contamination can occur in the linear terms of the wavefunction, but it has been shown[37] to sometimes be more reliable for certain transition states compared to spin adapted methods, i.e., RCCSD(T).[36] As detailed below, benchmark calculations were also performed with UHF-CCSD(T),[34] as well as ROHF-CCSDT, i.e., CCSD with full iterative triples[38] based on ROHF

orbitals. The latter calculations were carried out with the ACES II package,[39] the UHF-CCSD(T) calculations with GAUSSIAN98,[40] and all others with the MOLPRO suite of *ab initio* programs.[41]

III. Benchmark Calculations

A. The diatomics OH, HCl, and ClO

Some of the MRCI+Q (AVQZ′+*d* and CBS) spectroscopic constants and dissociation energies calculated for the diatomic 2-body potentials used in this work are shown in Table I, where they are also compared to experiment.[42] Extrapolation to the CBS limit via Eq.(1) is observed to have only a modest effect on the spectroscopic constants, but results in increases to D_e of 0.9 to 1.6 kcal/mol. It should be noted that the presence of the tight *d* function in the present calculations significantly improves the convergence of the ClO results towards the CBS limit (also towards experiment). While the MRCI+Q/CBS spectroscopic constants are in very good agreement with experiment, methods were explored to further improve upon these results, particularly in the case of the dissociation energies since these directly impact the reaction enthalpy of the final PES. One such method is the scaled external correlation (SEC) method,[13] whereby the correlation energy is scaled to reproduce experimental dissociation energies. While excellent results have been obtained with this procedure[43] by scaling to match experimental results, this prescription attempts to account for a large range of possible errors in the *ab initio* calculation, e.g., basis set incompleteness, inadequate correlation recovery, core-valence correlation, relativistic effects, etc. In the present work, where highly correlated wave functions are used with explicit basis set extrapolations, a purely *ab initio* method is more desirable. Lacking full CI (FCI) results, we have chosen to scale the MRCI+Q/CBS correlation energies by numerical factors based on CCSD(T) calculations, since the latter method exhibited excellent

agreement with experiment in preliminary benchmark calculations on these three diatomics, especially for the dissociation energies. The scale factor for diatomic AB is obtained as[13]

$$f_{\mathrm{AB}} = \frac{E_{\mathrm{AB}}^{\mathrm{CCSD(T)}}(r_e) - E_{\mathrm{AB}}^{\mathrm{CASSCF}}(r_e)}{E_{\mathrm{AB}}^{\mathrm{MRCI+Q}}(r_e) - E_{\mathrm{AB}}^{\mathrm{CASSCF}}(r_e)},$$

from R/UCCSD(T)/AVTZ′+*d* and MRCI+Q/AVTZ′+*d* calculations at the experimental equilibrium geometry of each diatomic. The scaled energies are calculated as

$$E_{\mathrm{AB}}^{s}(r) = E_{\mathrm{AB}}^{\mathrm{CASSCF}}(r) + f_{\mathrm{AB}}\left[E_{\mathrm{AB}}^{\mathrm{MRCI+Q}}(r) - E_{\mathrm{AB}}^{\mathrm{CASSCF}}(r)\right].$$

In addition to assuming the same basis set dependence between MRCI+Q and CCSD(T) for these species (and a geometry-independent scale factor), this scaling method also assumes that CCSD(T) includes the nondynamical correlation energy recovered in the CASSCF step preceding the MRCI+Q calculations, since the correlation energies in both cases are calculated relative to the CASSCF energy. The resulting scale factors are small (1.035 for OH, 1.044 for HCl, and 1.062 for ClO), but yield improved energetics and spectroscopic constants, as shown in Table I. The remaining errors can mainly be attributed to inaccuracies in the basis set extrapolation, as well as incomplete correlation energy recovery. Both core-valence correlation and scalar relativistic effects are expected to be relatively small for these species (see, e.g., Ref. 24).

Using the equilibrium dissociation energies from the "scaled" potentials, the energy change (without zero point energies) $\Delta V_{ab\ initio}$ for the O(^3P) + HCl → OH + Cl reaction is calculated to be –0.6 kcal/mol. While this appears to be in rather good agreement with the most recent experimental value of ΔV_{expt} = –0.57±0.12 kcal/mol (based on a re-evaluation of the D_e of OH[24]), this latter value contains substantial contributions from spin-orbit coupling[44] in O (0.22 kcal/mol), Cl (0.84 kcal/mol), and OH (0.11 kcal/mol) that are not included in the present *ab*

initio calculations. Removing these contributions (so as to permit a comparison of theory and experiment on an equal footing) results in $\Delta V_{expt} = -0.15$ kcal/mol. While future work will address spin-orbit effects at the *ab initio* level, a more accurate *ab initio* reaction energy was obtained in this work by using the *unscaled* MRCI+Q/CBS potential for HCl and the scaled potential for OH in the construction of the final OHCl PES (see below). That approach results in $\Delta V_{ab\ initio} = -0.07$ kcal/mol. The inclusion of zero-point vibrational effects yields an *ab initio* 0 K reaction enthalpy of +1.13 kcal/mol, which is in excellent agreement with the accurate experimental value without spin-orbit contributions of +1.19 ± 0.12 kcal/mol.

B. The reaction barrier

One of the critical aspects of the present work is to determine an accurate barrier height for the O+HCl reaction in order to construct a PES that will yield accurate rate constants and reliable dynamical information. Table II summarizes the results of numerous calculations at the MRCI+Q and CCSD(T) levels of theory for both the barrier height ($\Delta V^{\ddagger}$) and saddle point geometry. The latter was obtained either by polynomial fits to grids of *ab initio* energies or gradient optimizations using either ACESII[39] or MOLPRO.[41] Both methods were confirmed to yield essentially identical results. For both methods the convergence of $\Delta V^{\ddagger}$ and the saddle point geometry with basis set is smooth and the barrier height decreases with increasing basis set. The presence of tight *d* functions in the basis set slightly increases the barrier height, as can be observed by comparing the AVTZ and AV(T+*d*)Z results. While the MRCI+Q and R/UCCSD(T) geometries are very similar, the R/UCCSD(T) barrier height is generally about 1 kcal/mol smaller than the MRCI+Q value when a valence CAS reference function is used in the latter. As demonstrated below using much larger MRCI reference functions, the valence CAS-

MRCI+Q barrier height is certainly too high. The use of UHF orbitals in the CCSD(T) calculations is shown to only slightly effect the barrier height or geometry in comparison to the ROHF results. A much larger difference is observed between the R/UCCSD(T) and spin adapted RCCSD(T) results, with the latter yielding a barrier height larger by more than 1 kcal/mol with the AVDZ basis set. The barrier height and saddle point location from the fitted S4 surface of Ramachandran *et al*.[14] is also shown in Table II. Recall that this surface is a fit to SEC-scaled MRCI+Q/VTZ energies. The saddle point on the S4 surface is located later in the entrance channel with a barrier smaller by more than 1 kcal/mol than the R/UCCSD(T) results of this work. As mentioned earlier, recent QM calculations of thermal rate constants[18 19 20] have raised the possibility that the S4 barrier may be too low.

In order to further characterize the reaction barrier height, numerous single-point calculations were carried out at either the MRCI+Q or R/UCCSD(T) AVTZ′+*d* optimized geometry. While basis set extrapolation of the R/UCCSD(T) energies with the AV*n*Z′+*d* (*n*=D,T,Q) basis sets yielded a CBS limit barrier height of 10.9 kcal/mol, calculations with the more accurate AV*n*Z+*d* basis sets (i.e., the full AV*n*Z sets plus the additional tight *d*) yielded a CBS limit for the barrier of 10.82 kcal/mol (using TZ-5Z). Extrapolation of the R/UCCSD(T) series AVTZ through AV5Z yielded a very similar barrier height of 10.86 kcal/mol. Some other variants of coupled cluster theory were also investigated with the standard AVTZ basis set, namely UHF-based Brueckner doubles with perturbative triples, BD(T), and UHF-BD with perturbative triples and quadruples,[45] BD(TQ).[34] The former yielded a result for $\Delta V^{\ddagger}$ identical to UHF-CCSD(T) with the same basis set while the latter resulted in a barrier height lower by just 0.07 kcal/mol. Lastly, to investigate the impact of full iterative triples on the barrier height, calculations using the AVTZ basis were carried out with the CCSDT method using ROHF orbitals. The resulting

CCSDT barrier height was lower than the the CCSD(T) value by 0.60 kcal/mol. Hence, using the CCSD(T)/CBS value from above with the CCSDT/AVTZ result, a barrier height of 10.1 kcal/mol is *estimated* at the CCSDT/CBS level.

Of course CCSDT is still a single reference-based method and unfortunately the saddle point region has non-negligible multireference character as partially evidenced by the relatively large T1 amplitudes of just over 0.3 in both the CCSD(T) and CCSDT calculations. In addition, recent thermochemical calculations by Feller and co-workers[46] have demonstrated that CCSDT does not always yield a result that is closer to FCI than CCSD(T). To attempt to further benchmark the barrier height for this reaction, large-scale MRCI calculations were carried out with the AVTZ basis set. In these calculations, HF core orbitals were used in order to more accurately compare with the coupled cluster calculations and in addition the O 2*s* electrons were not correlated in order to make the calculations more amenable. The orbitals for the MRCI calculations were taken from the CI natural orbitals of a preceding valence-CAS MRCI. The reference space in the large MRCI calculation included a total of 17 a' orbitals and 6 a'' orbitals, which corresponded to all natural orbitals with occupations greater than 0.004 (a valence CAS reference includes 12 a' and 3 a'' orbitals). Reference configurations were then selected from the large set of configurations within this (17,6) space with a threshold of 0.001, yielding a total of 901 configurations for the saddle point geometry. The resulting internally contracted MRCI based on this reference function consisted of just over 46 million variational parameters and produced MRCI and MRCI+Q barrier heights of 12.17 and 10.34 kcal/mol, respectively. These represent a decrease in the barrier height compared to a valence CAS reference function of 3.1 and 2.3 kcal/mol for MRCI and MRCI+Q, respectively. An average of the MRCI and MRCI+Q values, 11.26 kcal/mol, is probably the most reliable estimate of the barrier height with this basis

set (with the O 2*s* electrons core) since the Davidson correction often has a tendency to overshoot with extended reference functions. This average is just 0.1 kcal/mol less than the CCSD(T) value of 11.37 kcal/mol with the same basis set. (At the CCSD(T) level of theory, freezing the O 2*s* electrons raises the barrier height by 0.68 kcal/mol.) Hence, these large-scale MRCI calculations appear to lend credence to the reliability of the CCSD(T) results, albeit the latter may be somewhat fortuitous.

Finally, two other effects were investigated as to their impact on the O+HCl barrier height, core-valence correlation and relativity. Calculations on both the reactants and saddle point were carried out with both valence-only and all-electrons correlated at the R/UCCSD(T)/cc-pwCVTZ level of theory. The change in the barrier height was calculated to be less than 0.01 kcal/mol. The effect of scalar relativity was assessed by using the Douglas-Kroll-Hess (DK) Hamiltonian[47] in CCSD(T)/AVTZ calculations (the *sp* part of the AVTZ basis set was recontracted in atomic DK calculations). In these calculations the barrier was calculated to decrease by just 0.1 kcal/mol. Lastly, in the case of spin-orbit coupling effects on the barrier height, the atomic zero-field splitting of the O atom, which is not included in the present *ab initio* calculations, will effectively increase the barrier by 0.22 kcal/mol. From these calculations, we obtain a reasonable estimate for the $^3A''$ barrier height, $\Delta V^{\ddagger}$, without spin-orbit coupling by taking the R/UCCSD(T)/CBS limit (10.82 kcal/mol) and applying the difference between CCSD(T) and the average of the large MRCI and MRCI+Q results (–0.1 kcal/mol), as well as the DK scalar relativistic correction (–0.1 kcal/mol). Therefore, we conclude that $\Delta V^{\ddagger}$ including all of these effects is then ~10.6 kcal/mol with a relatively conservative error estimate of ±0.5 kcal/mol. The greatest source of this uncertainty is probably the MRCI calibration but, at present, much larger calculations are not feasible with our current resources.

C. The reactant and product side van der Waals complexes

As previously shown with the S4 surface, van der Waals wells are present in both the entrance and exit channels of the O(^3P)+HCl reaction on the $^3A''$ PES. Table III shows the results of calculations at the MRCI+Q and R/UCCSD(T) levels of theory as a function of basis set for both van der Waals minima. The reactant well is linear with $^3\Sigma^-$ symmetry. Both CCSD(T) and MRCI+Q yield similar geometries and well depths for this species, namely a MRCI+Q/CBS limit equilibrium well depth of about –1.6 kcal/mol with respect to the O(^3P) + HCl asymptote, at bond lengths r_{OH} and r_{HCl} of 4.38a_0 and 2.41a_0, respectively. The CCSD(T) minimum is deeper by about 0.1 kcal/mol with a shorter r_{OH} distance of 4.23a_0.

Much larger differences between MRCI+Q and CCSD(T) are observed for the product side van der Waals species, which is sharply bent. The MRCI+Q/CBS well depth is –5.54 kcal/mol, again with respect to O(^3P)+HCl asymptote, while the CCSD(T) value is –3.46 kcal/mol. Inspection of the CI vector from the MRCI wave function clearly shows, however, that very strong multireference effects exist in this region of the PES with 3 coefficients being larger than 0.4 (0.66, 0.50, 0.40). Hence, the depth of this well is strongly influenced by interactions with higher $^3A''$ states. Therefore, the CCSD(T) results, or results from single reference methods in general, for this part of the PES are not expected to be particularly reliable.

IV. Potential Energy Surfaces

The reproducing kernel Hilbert space (RKHS) method,[48] which was introduced to the chemical physics community by Ho and Rabitz,[49 50] was used in combination with analytic two body functions in order to get an accurate representation of the PES's for the $^3A''$ and the $^3A'$ electronic states. The PES in both cases is represented by a many body expansion, as in

$$V(r_1,r_2,r_3) = V^{(1)} + \sum_{i=1}^{3} V^{(2)}(r_i) + V^{(3)}(r_1,r_2,r_3), \qquad (2)$$

where $(r_1, r_2, r_3) = (r_{OH}, r_{HCl}, r_{ClO})$. The constant $V^{(1)}$, representing the energy of the three atoms at infinite separation from each other, was subtracted from all *ab initio* energies so that the actual representation of the PES consists of only the second and third terms of Eq. (2).

A. Two body terms:

The two-body potentials for OH (scaled MRCI+Q/CBS), and HCl (unscaled MRCI+Q/CBS) were represented by the "extended Rydberg" function of Murrell and Sorbie,[51]

$$V(r) = -D_e\left(1 + a_1x + a_2x^2 + a_3x^3\right)e^{-a_1x}, \qquad (3)$$

where $x = r - r_e$. For OH, twelve points spanning the range $1.3a_0 \le r \le 2.4a_0$, were fitted to Eq. (3) with a root-mean-square (rms) error of 0.44 cm^{-1} (0.012 kcal/mol) and for HCl, nine points in the range $2.0a_0 \le r \le 3.1a_0$ were fitted with a rms error of 0.19 cm^{-1} (0.0055 kcal/mol). The strategy for these fits was as follows. First, the energies were fitted without restrictions on any of the parameters (D_e, r_e, a_i). Then, the r_e parameter was frozen, and D_e was set to (and frozen at) the value determined from the difference of the absolute minimum energy of the diatomic + atom system at the diatomic r_e value and that of the three separate atoms. A second fit was then obtained in which only the coefficients a_i were optimized.

In order to avoid unphysical behavior of the $^3A''$ PES at small O-H-Cl angles, the two-body potential for ClO on the PES's reported here is represented by a purely repulsive function. This is justifiable for the present purpose of studying the $O(^3P)$ + HCl → OH + Cl reaction, since the H + ClO channel is not physically accessible to the reactants until the total energy exceeds 42 kcal/mol.

B. The three-body term:

The majority of *ab initio* data, at the MRCI+Q/CBS level of theory, for both electronic states were obtained over a semi-structured grid of 70 points in (r_{OH}, r_{HCl}) space at θ_{OHCl} = 70, 90, 110, 130, 150, 170, and 180° (total of 490 points), spanning $1.35a_0 \le r_{OH} \le 6.0a_0$ and $1.75a_0 \le r_{HCl} \le 6.5a_0$. In order to accurately reproduce the properties of the entrance and exit channel van der Waals wells, additional scattered points (41 for the exit channel, spanning θ_{OHCl} in the range 51.8–81.8°, and 27 for the entrance channel well spanning 150–180°) were obtained in the vicinity of these stationary points for the $^3A''$ state. In order to model the long range behavior of the exit channel potential, especially in the vicinity of the exit channel van der Waals well, additional points were included at $r_{OH} = 1.84a_0$, θ_{OHCl} = 66.8°, and r_{HCl} in the range 7.28–$16.28a_0$.

Although various regularization methods[49] and other strategies have been suggested for obtaining physically reasonable fits through scattered data,[52] our approach has been to directly solve the linear system of equations resulting from the RKHS kernel representation of the three body potential. Perhaps because of this "simplified" approach, in order to get fits that are globally free of unphysical artifacts while reproducing the properties of the van der Waals wells as accurately as possible, we found it necessary to use two three body terms for the $^3A''$ state. One of these spans O-H-Cl angles smaller than 110° (251 points) while the other spans angles from 66.8° to 180° (521 points). A switching function is used to smoothly switch from one three-body term to the other over the range $75° \le \theta_{OHCl} \le 100°$ *after the fits are obtained.* The considerable overlap (in bond-angle space) of the two three body terms is essential to ensure a smooth transition from one to the other while maintaining accuracy in the switching region.

Since the $^3A'$ surface appears to be free of complicating features such as van der Waals minima, a single three-body term representing the above-mentioned grid of 490 points was used to obtain the fit.

The three body terms in each case are represented by a "composite" kernel obtained by the combination of distance-like kernels $q_1^{2,6}(x,x')$ and angle-like kernels $q_2^2(z,z')$,[49] as

$$V^{(3)}(x_j, y_j, z_j) = \sum_{i=1}^{N} Q^{6,6,2}(x_j, x_i; y_j, y_i; z_j, z_i)\ c_i;\ j = 1, 2, ..., N, \qquad (4)$$

where

$$Q^{l,m,n} = q_1^{2,l}(x, x')q_1^{2,m}(y, y')q_2^n(z, z'), \qquad (5)$$

$x = r_{OH}$, $y = r_{HCl}$, $z = (1 - \cos\theta_{OHCl})/2$. The choice of the z coordinate ensures the symmetry of the potential on either side of $\theta_{OHCl} = 180°$. For the $^3A''$ surface *only*, both $q_1^{2,6}$ kernels were multiplied by $(rr')^2$ ($r = x$ or y) effectively reducing the reciprocal power of the kernel. This modification leads to a better-conditioned system of equations in Eq. (4) and a smoother potential surface in the regions spanned by data. To counteract the rather slow asymptotic approach to zero of the modified distance-like kernels, the $^3A''$ three body terms were multiplied by a switching function that forces the three body term smoothly to zero for $r > 20a_0$, where $r^2 = r_{OH}^2 + r_{HCl}^2 + r_{ClO}^2$.

In all cases, the system of linear equations in Eq. (4) was solved using the singular value decomposition (SVD) procedure[53] to evaluate the expansion coefficients $\{c_i\}$. In order to avoid unphysical oscillations and kinks in certain regions of configuration space, we chose to set the threshold for singular eigenvalues in the SVD procedure high enough to reject the smallest singular eigenvalue. This reduced the rank of the resulting kernels by 1 in each case, and introduced small, but non-zero, rms errors into the fits. The rms error for the $^3A''$ surface is ΔV_{rms}

= 0.0363 kcal/mol and the largest absolute deviation from an *ab initio* energy is $|\Delta V|_{max}$ = 0.3437 kcal/mol. Analogous numbers for the $^3A'$ surface are ΔV_{rms} = 0.0037 kcal/mol and $|\Delta V|_{max}$ = 0.0316 kcal/mol.

Finally, the two three-body terms $V^{(3)}(x,y,z)$ for the $^3A''$ surface were multiplied by a scaling factor $f < 1.00$ so that the reaction barrier on the PES closely matched the best estimate value of 10.60 kcal/mol established by the benchmark CCSD(T) and MRCI calculations (see above). This also resulted in a reduction of the collinear barrier on the $^3A''$ surface. Since the $^3A'$ and $^3A''$ surfaces are degenerate at collinear configurations, the three-body term for the $^3A'$ surface was also scaled in the same manner so as to make it degenerate with the scaled $^3A''$ surface at its collinear saddle point. By trial and error, the scale factors were found to be 0.9807 and 0.9818 for the $^3A''$ and $^3A'$ surfaces, respectively.

V. Discussion

Three views of the $^3A''$ surface in (r_{OH},r_{HCl}) space are shown in Fig. 1. In each view, θ_{OHCl} is frozen at the specified value, which corresponds to (a) the bent saddle point (135.9°), (b) the product side van der Waals well (68.6°), and (c) the reactant side van der Waals well (180°). It is clear from these representations that the RKHS procedure yields a smooth, well-behaved potential surface for this system. A further check on the smoothness of the surface was provided by the quantum mechanical (QM) reactive scattering calculations described in the following paper.[25] Initial versions of the $^3A''$ surface produced very noisy cumulative reaction probabilities (CRP's) as a function of scattering energy. A careful analysis of the surface topology revealed that the switching functions connecting the two three-body terms had to be adjusted in order to yield a smooth and physical surface.

The angular dependence of the $^3A''$ and $^3A'$ surfaces at their *respective* saddle point bond lengths are shown in Figure 2. The angular dependence of the $^3A''$ surface is very similar to that of the S4 surface (see Ref. 14). The angular dependence of the $^3A'$ surface is unremarkable, but it is clear that the minimum energy saddle point on this surface lies at a collinear geometry. Also shown, as a dashed line, is the angular dependence of the $^3A''$ potential at the bond lengths of the $^3A'$ surface's collinear saddle point, which shows that the two surfaces are nearly degenerate at $\theta_{OHCl} = 180°$.

The properties of the $^3A''$ saddle point are summarized in Table IV. Note that the scaled barrier height is in excellent agreement, by design, with the best estimate from benchmark calculations (see above) of 10.6 kcal/mol. The collinear barrier on the $^3A''$ surface is located further into the exit channel than the bent saddle point, and is degenerate with the saddle point on the $^3A'$ surfaces surface. After the $^3A''$ surface was scaled as described above, this degeneracy property was used to determine the scale factor for the $^3A'$ surface. In both cases, scaling reduces the barrier by less than 1.4 kcal/mol and introduces only moderate changes in the saddle point locations.

It was mentioned earlier that one of the shortcomings of the S4 surface was that the reaction barrier appeared to be too narrow, in the sense of permitting too much tunneling, which results in low temperature thermal rate coefficients that are higher than those calculated on the KSG surface,[18 19 20] in spite of the fact that the S4 barrier is 1.3 kcal/mol higher. Figure 3 shows the variation of the potential energy along the respective minimum energy paths (MEPs) for the S4 and the present $^3A''$ surfaces. It is clear that the PES presented here has a broader barrier. Given the fact that both these surfaces are based on similar approaches to *ab initio* calculations (both

use MRCI+Q energies, but use different basis sets), it is reasonable to conclude that the narrow barrier on the S4 surface is an artifact of the SEC scaling employed in that case.

The shape of the barrier on the present $^3A''$ surface is somewhat unusual however, in the range $0.5 \le s \le 2.0$. In this range of the reaction coordinate, the MEP passes through θ_{OHCl} in the range 137° to 90°. Because of the distribution of *ab initio* points at 20° intervals (see Section IV.B), the possibility that this is an artifact of the fit cannot be ruled out. However, the shoulder becomes more pronounced if the 70-point grid in (r_{OH},r_{HCl}) space is generated at intermediate θ_{OHCl} by interpolation from a subset of data. The shoulder is also present in a less pronounced form in an *interpolation* using the regular grid of 490 points described in Section IV.B with or without the modification to the distance-like kernel mentioned there.

We now turn attention to the van der Waals (vdW) wells on the $^3A''$ surface. The low energy resonances in the S4 cumulative reaction probability have recently been attributed to the presence of wells similar to these.[54] Panels (b) and (c) of Figure 1 show the locations of the exit and entrance channel wells, respectively, in (r_{OH},r_{HCl}) space. The locations of the minima and the vibrational frequencies of these wells on the PES are compared to those calculated from locally interpolated (i.e., fits with zero rms error) MRCI+Q/CBS energies in Table V.

The reactant-side well, corresponding to the O–HCl species, lies at $\theta_{OHCl} = 180°$ and has a relative energy of –1.57 kcal/mol with respect to the O + HCl asymptote prior to scaling. The scaling of the PES decreases its depth slightly, to –1.54 kcal/mol. The equilibrium geometry of this species and the vibrational frequencies calculated from the fit (unscaled and scaled) are in reasonably good agreement with the results obtained directly from *ab initio* calculations. The three-atom system is best described as the electronegative O atom hydrogen-bonded to the HCl molecule.

The product-side vdW well is much deeper, with a relative energy of –5.54 kcal/mol with respect to the O + HCl asymptote prior to scaling. Panel (a) of Figure 4 shows the contours of the $^3A''$ surface with the Cl–O distance frozen at $4.24a_0$, the value that corresponds to the exit channel well minimum, and an expanded view of the well region is shown in panel (b). The scaling of the PES decreases the depth of the well to –5.22 kcal/mol with respect to the reactant asymptote. The nature of the bonding in the case of the exit channel vdW complex appears to be more complex than simply Cl hydrogen-bonded to the hydrogen end of the OH molecule. The depth of the well and the sharply bent geometry, which puts the Cl in closer proximity of the O atom than in the case of the collinear entrance channel well, indicate that there may be interactions between the Cl and the O atom as well. The Cl-O distance turns out to be about $4.24a_0$ at the well minimum, which represents an increase in bond length by about 40% compared to the equilibrium bond length of the ClO molecule (see Table I).

High level calculations of the $^3A''$ barrier height and width have been recently reported by Skokov et al.[18] These calculations were done along the minimum energy path (MEP) of the S4 surface using the Multi-Coefficient Gaussian-3 (MCG3) method.[55,56] Two versions of this method, "2s" which explicitly includes spin-orbit effects,[57] and "2m" which includes them implicitly,[58] were employed. These two variants yielded barrier heights of 9.65 and 9.56 kcal/mol, respectively. These are lower than the barrier height predicted by large scale coupled cluster and multi-reference calculations in this work, but the MCG3 as well as the present work predict thicker barriers than the S4 surface, which would lead to significantly lower tunneling probabilities at a given scattering energy and, therefore, smaller rate coefficients at low temperature than those obtained using the S4 surface.

A recent publication[26] has also reported calculations on the saddle points and local minima of the two electronic states investigated here. Those calculations identified the relevant geometries at the B3LYP/6-311+G(3*df*,2*p*) level of theory followed by single point evaluations of the relative energies using the G2M, MP2, MP4, and CCSD(T) methods with a slightly larger [6-311++G(3*df*,2*p*)] basis set. One set of calculations for the saddle points and the exit channel vdW complex were also carried out at the CCSD(T)/6-311+G(3*df*,2*p*)//CCSD(T)/6-31+G(*d*,*p*) level of theory. The bent $^3A''$ barrier heights predicted by the G2M (9.19 kcal/mol), CCSD(T)/6-311++G(3*df*,2*p*)//B3LYP/6-311+G(3*df*,2*p*) (8.96 kcal/mol) and CCSD(T)/6-311+G(3*df*,2*p*)//CCSD(T)/6-31+G(*d*,*p*) (9.63 kcal/mol) calculations of Ref. 26, all of which include zero point energy (zpe) contributions, are comparable to our own MRCI+Q/CBS results (the $\Delta V_0^{\ddagger}$ values in Table IV), which are 8.83 kcal/mol for the scaled and 10.09 kcal/mol for the unscaled surfaces. The CCSD(T)//B3LYP collinear $^3A'$ barrier height of 11.05 kcal/mol and the CCSD(T)//CCSD(T) value of 11.54 kcal/mol reported in Ref. 26 are also comparable to the scaled MRCI+Q/CBS value of 11.97 kcal/mol. Ref. 26 also reports that a third saddle point on the $^3A''$ surface, at θ_{OHCl} = 164.6° was identified at the B3LYP level of theory but its presence could not be confirmed at higher levels of theory. Our own calculations do not indicate the presence of a third $^3A''$ saddle point between the bent minimum energy saddle point at ~135° and the second order collinear saddle point at 180°. It is worth pointing out that the B3LYP method reports barrier heights of 0.56 and 2.81 kcal/mol for the bent and collinear saddle points,[26] which are in considerable error. Hence, this extra transition state is most probably an artifact of this method.

The present work and Ref. 26 report considerably different depths for the exit channel vdW well and much smaller differences (< 0.50 kcal/mol) for the entrance channel well. All of the

well depths reported in Ref. 26, which include zpe contributions, are larger in magnitude than the ΔV_0 values tabulated in Table V. As noted earlier in Section II, we believe that this is just reflective of the strong multireference effects that are important in the regions surrounding the exit channel vdW well of this system, which makes the single reference methods used in Ref. 26 less reliable in this region. It is noteworthy that a well-depth of –15.10 kcal/mol is reported for the exit channel well at the B3LYP/6-311+G(3*df*,2*p*) level of theory which, like the barrier height with this method, is greatly in error. In addition, the CCSD(T)/6-311++G(3*df*,2*p*)// B3LYP/6-311+G(3*df*,2*p*) well depth of –7.31 kcal/mol (including zpe) reported in Ref. 26 is also too deep. It differs considerably from the R/UCCSD(T)/AVQZ′+d well-depth reported in the present work (–1.25 kcal/mol, after correcting for zpe), as well as the unscaled (–3.36 kcal/mol) and scaled (–2.97 kcal/mol) ΔV_0 values obtained from the PES (see Table V). Some of these differences could arise from the use in Ref. 26 of B3LYP harmonic frequencies, unrestricted HF (UHF) orbitals, as well as larger basis set superposition errors from their choice of basis set.

VI. Summary

This paper presents accurate potential energy surfaces for the $^3A''$ and $^3A'$ electronic states of the O-H-Cl system spanning those regions of configuration space that are relevant for the study of the O(^3P) + HCl reaction, at total energies less than 40 kcal/mol. The *ab initio* energies that form the basis for these PES's were obtained at the MRCI+Q/CBS level of theory. By extensive calculations using various single and multiple reference methods and fairly large basis sets, we have established that the potential energy barrier for this reaction on the $^3A''$ surface is about 10.6 kcal/mol. This value is more than 2 kcal/mol higher than the barrier on the KSG surface,[7] and almost 1 kcal/mol higher than the S4 surface.[14] The reaction barrier calculated in the present

work also appears to be broader than that on the S4 surface. In these respects, we believe that the present work is a substantial improvement over the earlier attempts to construct an accurate potential energy surface for the $^3A''$ electronic state for this system. This work also reports the first potential energy surface for the $^3A'$ state based on *ab initio* calculations.

The van der Waals wells found in the entrance and exit channels of the S4 surface, which was based on SEC-scaled MRCI+Q/cc-pVTZ energies, have been confirmed by the present work. It appears that the entrance channel minimum is better described as the oxygen atom hydrogen bonded to the HCl molecule while the structure and bonding of the product side well appears to be much more complex.

In contrast to the $^3A''$ surface, the topolgy of the $^3A'$ surface appears to be quite unremarkable. In an attempt to approximately account for the contributions from the $^3A'$ surface to the high temperature thermal rate constants of the O(^3P) + HCl reaction, KSG[7] used the reaction probabilities from the LEPS surface of Persky and Broida,[59] shifted in energy by appropriate amounts. The PES for this electronic state obtained in this work appears to justify their approach.

It is possible that this work has extended the types of systems for which PES's have been constructed using the RKHS method. The RKHS method has up to now, proved to be quite successful in generating potential surfaces for three atom systems of the A_3 (H_3^+ [49]), AB_2 (OH_2,[52] [60] NH_2,[50] [61], SH_2[62]), or ABC (NeCO[63]) type that have fairly deep minima in the three-body region. In the present work, we have applied the method to two electronic states which have fairly high reaction barriers in the three-body interaction region, one of which also has a rather deep van der Waals well in the exit channel at a very sharp A-B-C bond angle. It can be argued that the former cases, which represent potential surfaces for fairly stable triatomic species, are

easier to construct using many body type expansions because the sum of the two body terms produce the deep minimum in approximately the correct region of configuration space. The three body term, then, only has to provide (minor) corrections and adjustments to the depth and shape of this well. In contrast, in the present cases, the three body term needs to not only overcome the deep minimum, but also "build" the reaction barrier on top of the two-body well. This means that the three body term must go from a very large positive value in the three-body interaction region to vanishingly small values asymptotically and at small bond lengths. It is possible that the numerical difficulties we encountered with the RKHS kernels in the present work are a direct consequence of this, forcing us to resort to multiple three-body terms and rank deficient "composite" kernels.

Working with rank deficient matrices in the SVD procedure does indeed raise the possibility that the solution obtained is not unique, and that it may be sensitive to small perturbations. However, similar comments can be made about any fit to *ab initio* data using polynomials in various coordinates. So, in one sense, reducing the rank of the kernel is equivalent to moving from interpolating the data to obtaining a reasonably good fit to it. The quality of such fits are usually estimated by calculating the root-mean-square error. In this regard, it is noteworthy that the root-mean-square errors reported here, 0.0363 and 0.0037 kcal/mol respectively, for the $^3A''$ and $^3A'$ surfaces, are among the lowest for PES's available for dynamical calculations on small molecular systems.

The accurate prediction of reaction barrier heights may be one of the greatest challenges facing modern quantum chemistry. In the present work, we have used the MRCI+Q method in order to get *ab initio* energies that span large enough portions of configuration space so that potential energy surfaces for reaction dynamics studies can be constructed. At the same time, we

have performed large scale MRCI and CCSD(T) benchmark calculations in the saddle point region to provide us with a better estimate of the reaction barrier height. Finally, we chose to scale the potential energy surface obtained by fitting MRCI+Q/CBS energies to reproduce the reaction barrier predicted on the basis of these benchmark calculations. The success of this approach can be established only by verifying whether accurate quantum mechanical thermal rate coefficients calculated on these potential energy surfaces provide a good description of the available experimental data. That is the subject of the following paper.[25]

Acknowledegements

The authors acknowledge very useful discussions and exchange of information with Professor Joel M. Bowman and Dr. Tiao Xie during the course of this work. We acknowledge the support of the National Science Foundation (CHE-9501262 to KAP and CHE-9712764 to BR).

Table I. Properties of the calculated two body potentials compared to experimental values. Dissociation energies are in kcal/mol, bond lengths in bohr, and other quantities in cm^{-1}.

	D_e[(a)]	r_e	ω_e	$\omega_e x_e$	B_e	α_e
			HCl ($^1\Sigma^+$)			
MRCI+Q/AVQZ′+*d*	106.0	2.4100	2999.0	52.6	10.5809	0.304
MRCI+Q/CBS	106.9	2.4103	2999.9	52.8	10.5778	0.304
Scaled[(b)]	107.6	2.4096	3003.7	52.7	10.5843	0.304
Experiment[(c)]	107.32	2.4086	2990.9	52.8	10.5934	0.307
			OH ($^2\Pi$)			
MRCI+Q/AVQZ′+*d*	105.3	1.8330	3746.0	85.1	18.8986	0.719
MRCI+Q/CBS	106.2	1.8298	3754.6	85.3	18.9648	0.726
Scaled[(b)]	107.0	1.8295	3758.3	85.6	18.9700	0.721
Experiment[(c)]	107.17[(d)]	1.8324	3737.8	84.9	18.9108	0.724
			ClO ($^2\Pi$)			
MRCI+Q/AVQZ′+*d*	60.5	2.9835	833.0	5.2	0.6162	0.0060
MRCI+Q/CBS	62.1	2.9749	838.1	5.2	0.6198	0.0059
Scaled[(b)]	63.7	2.9691	844.9	5.2	0.6222	0.0059
Experiment[(c)]	65.26	2.9662	853.8	5.5	0.6234	0.0058

(a) Atomic (Ref. 44) and molecular SO effects have been removed from the experimental values. The experimental D_e values including SO are (in kcal/mol) 106.48 (HCl), 107.05 (OH), and 64.64 (ClO).

(b) See the text.

(c) Reference 42 unless otherwise noted.

(d) Reference 24.

Table II. Benchmark calculations of the barrier height (kcal/mol) and optimal geometry (bohr and deg.) of the transition state on the $^3A''$ surface.

Method	$\Delta V^{\ddagger}$	r_{OH}	r_{HCl}	θ_{OHCl}
MRCI+Q/[(a)]				
AVDZ	11.92	2.337	2.764	133.4
AVTZ	11.66	2.335	2.732	134.7
AV(T+*d*)Z	12.20	2.338	2.729	134.8
AVDZ+*d*	12.81	2.323	2.763	133.1
AVTZ′+*d*	12.30	2.327	2.733	134.8
AVQZ′+*d*	12.11	2.331	2.729	133.7
R/UCCSD(T)/				
AVDZ	11.36	2.330	2.764	135.1
AVTZ	10.69	2.329	2.730	136.4
AV(T+*d*)Z	10.99	2.323	2.731	136.2
AVDZ+*d*	12.19	2.315	2.763	134.7
AVTZ′+*d*	11.43	2.322	2.732	136.2
AVQZ′+*d*	11.11	2.328	2.728	135.1
UHF-CCSD(T)/				
AVDZ	11.43	2.322	2.773	134.5
RCCSD(T)/				
AVDZ	12.66	2.303	2.781	130.3
S4[(b)]	9.78	2.424	2.664	131.6

(a) Valence CAS reference, see the text.

(b) Reference 14.

Table III. Properties of the $^3A''$ reactant side and product side van der Waals wells as a function of basis set and level of theory.

Method	E_{min} (a.u.)	$\Delta V^{(a)}$ (kcal/mol)	r_{OH} (a_o)	r_{HCl} (a_o)	θ_{OHCl} (deg.)	ω_s cm^{-1}	ω_a cm^{-1}	ω_b cm^{-1}
			O–HCl					
MRCI+Q/								
AVDZ+*d*	–535.212294	–1.93	4.276	2.432	180.	93.9	2963.6	207.4
AVTZ′+*d*	–535.316383	–1.69	4.386	2.415	180.	111.5	3071.2	219.1
AVQZ′+*d*	–535.354241	–1.62	4.383	2.411	180.	108.2	3016.8	207.7
R/UCCSD(T)/								
AVDZ+*d*	–535.214092	–2.08	4.227	2.434	180.	100.6	2947.4	212.2
AVTZ′+*d*	–535.321712	–1.79	4.264	2.417	180.	94.2	2960.0	196.9
AVQZ′+*d*	–535.361053	–1.72	4.228	2.417	180.	94.4	2953.7	187.4
			Cl–OH					
MRCI+Q/								
AVDZ+*d*	–535.215774	–4.12	1.859	4.720	66.1	3633.1	257.7	584.8
AVTZ′+*d*	–535.321102	–4.65	1.843	4.692	66.8	3674.1	239.1	541.5
AVQZ′+*d*	–535.359914	–5.18	1.840	4.642	66.7	3730.4	259.3	555.4
R/UCCSD(T)/								
AVDZ+*d*	–535.213582	–1.76	1.861	4.807	65.3	3628.3	159.4	529.1
AVTZ′+*d*	–535.322726	–2.42	1.847	4.953	66.8	3683.6	105.1	506.8
AVQZ′+*d*	–535.363185	–3.06	1.843	4.784	66.6	3679.8	138.2	446.9

(a) With respect to the O + HCl asymptote.

Table IV. Properties of the minimum energy saddle points on the RKHS $^3A''$ and $^3A'$ surfaces. (Distances in Bohr, angles in degrees, energies in kcal/mol, relative to the O + HCl minimum, and frequencies in cm^{-1}.)

	$^3A''$ (unscaled)	$^3A''$ (scaled)	$^3A'$ (unscaled)	$^3A'$ (scaled)
$r_{OH}^{\ddagger}$	2.3393	2.3437	2.2473	2.2466
$r_{HCl}^{\ddagger}$	2.7247	2.7107	2.7932	2.7822
$\theta_{OHCl}^{\ddagger}$	135.22	135.95	180.0	180.0
$\Delta V^{\ddagger}$	11.86	10.60	15.15	13.77
$\Delta V_0^{\ddagger}$ (a)	10.09	8.83	13.48	11.97
$\omega_b^{\ddagger}$	318.31	325.28	492.80	491.84
$\omega_s^{\ddagger}$	1443.05	1434.80	669.75	627.35
$\omega_a^{\ddagger}$	1912.62i	1840.67i	2194.64i	2142.45i

(a) Including local and reactant zero-point energies.

Table V. Properties of the van der Waals minima on the on the RKHS $^3A''$ surface compared to the underlying *ab initio* (MRCI+Q/CBS) properties. (Distances in Bohr, angles in degrees, energies in kcal/mol, and frequencies in cm^{-1}.)

	$^3A''$ (MRCI+Q/CBS)	$^3A''$ (unscaled)	$^3A''$ (scaled)
		O–HCl	
r_{OH}	4.2583	4.2861	4.2450
r_{HCl}	2.4167	2.4169	2.4176
θ_{OHCl}	180.0	180.0	180.0
ΔV	–1.58	–1.57	–1.54
ΔV_0 [(a)]	–1.06	–1.20	–1.20
ω_s	119.36	116.06	106.03
ω_b	192.89	148.36	145.88
ω_a	3048.33	3010.61	3010.03
		Cl–OH	
r_{OH}	1.8373	1.8372	1.8366
r_{HCl}	4.6138	4.5989	4.5535
θ_{OHCl}	66.63	66.99	68.57
ΔV	–5.54	–5.54	–5.22
ΔV_0 [(a)]	–3.32	–3.36	–2.97
ω_a	271.33	268.29	262.77
ω_b	577.72	544.06	605.79
ω_s	3703.78	3689.23	3702.87

(a) Including local and reactant zero-point energies.

References

[1] R. D. Brown and I. W. M. Smith, Int. J. Chem. Kinet. **10**, 1 (1978).

[2] A. Persky and M. Broida, J. Chem. Phys. **81**, 4352 (1984).

[3] H. Koizumi and G. C. Schatz, Int. J. Quantum Chem. **23**, 137 (1989).

[4] H. Koizumi and G. C. Schatz, in *Advances in Molecular Vibration and Collision Dynamics*, edited by J. M. Bowman and M. A. Ratner (JAI, Greenwich, CT, 1990).

[5] S. C. Park, H. Nakamura, and A. Ohsaki, J. Chem. Phys. **92**, 6538 (1990).

[6] M. S. Gordon, K. K. Baldridge, D. E. Bernholdt, and R. J. Bartlett, Chem. Phys. Lett. **158**, 189 (1989).

[7] H. Koizumi, G. C. Schatz, and M. S. Gordon, J. Chem. Phys. **95**, 6421 (1991).

[8] K. Moribayashi and H. Nakamura, J. Phys. Chem. **99**, 15410 (1995).

[9] W. H. Thompson and W. H. Miller, J. Chem. Phys. **106**, 142 (1997); **107**, 2164 (1997).

[10] B. Poirier, J. Chem. Phys. **108**, 5216 (1998).

[11] F. Matzkies and U. Manthe, J. Chem. Phys. **110**, 88 (1999).

[12] F. J. Aoiz, L. Bañares, J. F. Castillo, M. Menéndez, and J. E. Verdasco, PCCP **1**, 1149 (1999).

[13] F. B. Brown and D. G. Truhlar, Chem. Phys. Lett. **117**, 307 (1985).

[14] B. Ramachandran, E. A. Schrader, III, J. Senekowitsch, and R. E. Wyatt, J. Chem. Phys. **111**, 3862 (1999).

[15] B. Ramachandran, J. Chem. Phys. **112**, 3680 (2000).

[16] R. J. Rakestraw, K. G. McKendrick, and R. N. Zare, J. Chem. Phys. **87**, 7341 (1987); R. Zhang, W. J. van der Zande, M. J. Bronikowski, and R. N. Zare, J. Chem. Phys. **94**, 2704 (1991).

[17] D. G. Truhlar, A. D. Issacson, and B. C. Garrett, in *Theory of Chemical Reaction Dynamics*, edited by M. Baer (CRC Press, Boca Raton, FL, 1985), Vol. **4**, p.65.

[18] S. Skokov, S. Zou, J. M. Bowman, T. C. Allison, D. G. Truhlar, Y. Lin, B. Ramachandran, B. C. Garrett, and B. J. Lynch, J. Phys. Chem. A **105**, 2298 (2001).

[19] S. Skokov, T. Tsuchida, S. Nanbu, J. M. Bowman, and S. K. Gray, J. Chem. Phys. **113**, 227 (2000).

[20] K. Nobusada, H. Nakamura, Y. Lin, and B. Ramachandran, J. Chem. Phys. **113**, 1026 (2000).

[21] T. H. Dunning, Jr., J. Chem. Phys. **90**, 1007 (1989); R. A. Kendall, T. H. Dunning, Jr., and R. J. Harrison, J. Chem. Phys. **96**, 6796 (1992); D. E. Woon and T. H. Dunning, Jr., J. Chem. Phys. **98**, 1358 (1993); T. H. Dunning, Jr. J. Phys. Chem. **104**, 9062 (2000).

[22] K. A. Peterson, D. E. Woon, and T. H. Dunning, Jr., J. Chem. Phys. **100**, 7410 (1994).

[23] K. A. Peterson, S. Skokov, and J. M. Bowman, J. Chem. Phys. **111**, 7446 (1999); K. A. Peterson, J. Chem. Phys. **113**, 4598 (2000); K. A. Peterson, B. A. Flowers, and J. S. Francisco, J. Chem. Phys. **115** (16), 7513 (2001); D. Feller and K. A. Peterson, J. Chem. Phys. **110**, 8384 (1999).

[24] B. Ruscic, A. F. Wagner, L. B. Harding, R. L. Asher, D. Feller, D. A. Dixon, K. A. Peterson, Y. Song, X. Qian, C.-Y. Ng, J. Liu, W. Chen, and D. W. Schwenke, J. Phys. Chem. A **106**, 2727 (2002).

[25] T. Xie, J. M. Bowman, K. A. Peterson, and B. Ramachandran, J. Chem. Phys. **xxx**, yyyy (2003) (the following paper).

[26] C-C. Hsiao, Y-P. Lee, N. S. Wang, J. H. Wang, and M. C. Lin, J. Phys. Chem. A **106**, 10231 (2002).

[27] S. Skokov, K. A. Peterson, and J. M. Bowman, J. Chem. Phys. **109**, 2662 (1998); K. A. Peterson, S. Skokov, and J. M. Bowman, J. Chem. Phys. **111**, 7446 (1999).

[28] T. H. Dunning, Jr., J. Chem. Phys. **90**, 1007 (1989); D. E. Woon and T. H. Dunning, Jr., J. Chem. Phys. **98**, 1358 (1993).

[29] R. A. Kendall, T. H. Dunning, Jr., and R. J. Harrison, J. Chem. Phys. **96**, 6796 (1992); D. E. Woon and T. H. Dunning, Jr., J. Chem. Phys. **98**, 1358 (1993).

[30] T. H. Dunning, Jr., K. A. Peterson, and A. K. Wilson, J. Chem. Phys. **114**, 9244 (2001) and references therein.

[31] H.-J. Werner and P. J. Knowles, J. Chem. Phys. **89**, 5803 (1988); P. J. Knowles and H.-J. Werner, Chem. Phys. Lett. **145**, 514 (1988).

[32] S. R. Langhoff and E. R. Davidson, Int. J. Quantum Chem. **8**, 61 (1974); M. R. A. Blomberg and P. E. M. Siegbahn, J. Chem. Phys. **78**, 5682 (1983); J. Simons, J. Phys. Chem. **93**, 626 (1989).

[33] L. M. Cheung, K. R. Sundberg, and K. Ruedenberg, Int. J. Quantum Chem. **16**, 1103 (1979).

[34] K. Raghavachari, G. W. Trucks, J. A. Pople, and M. Head-Gordon, Chem. Phys. Lett. **157**, 479 (1989).

[35] G. E. Scuseria, Chem. Phys. Lett. **176**, 27 (1991); J. D. Watts, J. Gauss, and R. J. Bartlett, J. Chem. Phys. **98**, 8718 (1993).

[36] P. J. Knowles, C. Hampel, and H.-J. Werner, J. Chem. Phys. **99**, 5219 (1994).

[37] K. A. Peterson and T. H. Dunning, Jr., J. Phys. Chem. **101**, 6280 (1997).

[38] J. Noga and R. J. Bartlett, J. Chem. Phys. **86**, 7041 (1987).

[39] ACES II is a program product of the Quantum Theory Project, University of Florida. Authors: J.F. Stanton, J. Gauss, J.D. Watts, M. Nooijen, N. Oliphant, S.A. Perera, P.G. Szalay, W.J. Lauderdale, S.R. Gwaltney, S. Beck, A. Balková, D.E. Bernholdt, K.-K. Baeck, P. Rozyczko, H. Sekino, C. Hober, and R.J. Bartlett. Integral packages included are VMOL (J. Almlöf and P.R. Taylor); VPROPS (P. Taylor); ABACUS (T. Helgaker, H.J. Aa. Jensen, P. Jørgensen, J. Olsen, and P.R. Taylor). AcesII (v3.0) (1999).

[40] Gaussian 98, Revision A.11.2, M. J. Frisch, G. W. Trucks, H. B. Schlegel, G. E. Scuseria, M. A. Robb, J. R. Cheeseman, V. G. Zakrzewski, J. A. Montgomery, Jr., R. E. Stratmann, J. C. Burant, S. Dapprich, J. M. Millam, A. D. Daniels, K. N. Kudin, M. C. Strain, O. Farkas, J. Tomasi, V. Barone, M. Cossi, R. Cammi, B. Mennucci, C. Pomelli, C. Adamo, S. Clifford, J. Ochterski, G. A. Petersson, P. Y. Ayala, Q. Cui, K. Morokuma, N. Rega, P. Salvador, J. J. Dannenberg, D. K. Malick, A. D. Rabuck, K. Raghavachari, J. B. Foresman, J. Cioslowski, J. V. Ortiz, A. G. Baboul, B. B. Stefanov, G. Liu, A. Liashenko, P. Piskorz, I. Komaromi, R. Gomperts, R. L. Martin,

D. J. Fox, T. Keith, M. A. Al-Laham, C. Y. Peng, A. Nanayakkara, M. Challacombe, P. M. W. Gill, B. Johnson, W. Chen, M. W. Wong, J. L. Andres, C. Gonzalez, M. Head-Gordon, E. S. Replogle, and J. A. Pople, Gaussian, Inc., Pittsburgh PA, 2001. Gaussian98 (1998).

[41] MOLPRO is a package of *ab initio* programs written by H.-J. Werner and P.J. Knowles with contributions from J. Almlöf, R.D. Amos, A. Bernhardsson, A. Berning, P. Celani, D.L. Cooper, M.J.O. Deegan, A.J. Dobbyn, F. Eckert, S.T. Elbert, C. Hampel, G. Hetzer, T. Korona, R. Lindh, A.W. Lloyd, S.J. McNicholas, F.R. Manby, W. Meyer, M.E. Mura, A. Nicklass, P. Palmieri, K.A. Peterson, R.M. Pitzer, P. Pulay, G. Rauhut, M. Schütz, H. Stoll, A.J. Stone, R. Tarroni, P.R. Taylor, T. Thorsteinsson. Molpro2000 (2000).

[42] K. P. Huber and G. Herzberg, *Molecular Spectra and Molecular Structure IV. Constants of Diatomic Molecules*. (Van Nostrand, Princeton, 1979).

[43] D. W. Schwenke, R. Steckler, F. B. Brown, and D. G. Truhlar, J. Chem. Phys. **84**, 5706 (1986); C. H. Yu, D. J. Kouri, M. Zhao, D. G. Truhlar, and D. W. Schwenke, Chem. Phys. Lett. **157**, 491 (1989); S. L. Mielke, D. W. Schwenke, S. C. Tucker, R. Steckler, F. B. Brown, G. C. Lynch, and D. G. Truhlar, J. Chem. Phys. **90**, 3110 (1989); G. C. Lynch, R. Steckler, D. W. Schwenke, A. J. C. Varandas, D. G. Truhlar, and B. C. Garrett, J. Chem. Phys. **94**, 7136 (1991); S. L. Mielke, G. C. Lynch, D. G. Truhlar, and D. W. Schwenke, Chem. Phys. Lett. **213**, 10 (1993); 217, 387 (1994) (E); H. Zhang, B. Ramachandran, J. Senekowitsch, and R. E. Wyatt, J. Mol. Struct. (Theochem) **487**, 75 (1999).

[44] C. E. Moore, *Atomic Energy Levels*. (NSRDS-NBS 35, Office of Standard Reference Data, National Bureau of Standards, Washington, D.C., 1971).

[45] N. C. Handy, J. A. Pople, M. Head-Gordon, K. Raghavachari, and G. W. Trucks, Chem. Phys. Lett. **164**, 185 (1989).

[46] D. Feller, J. Chem. Phys. 111, 4373 (1999); D. Feller and J. A. Sordo, J. Chem. Phys. 112, 5604 (2000); D. Feller and J. A. Sordo, J. Chem. Phys. 113, 485 (2000).

[47] M. Douglas and N. M. Kroll, Ann. Phys. (New York) **82**, 89 (1974); G. Jansen and B. A. Hess, Phys. Rev. A **39**, 6016 (1989).

[48] *Reproducing Kernel Hilbert Spaces: Applications in Statistical Signal Processing*, edited by H. Weinert (Hutchinson Ross, Stroudsburg, 1982).

[49] T. -S. Ho and H. Rabitz, J. Chem. Phys. **104**, 2584 (1996).

[50] T. -S. Ho, T. Hollebeek, and H. Rabitz, J. Chem. Phys. **106**, 7223 (1997).

[51] J. N. Murell and K. S. Sorbie, J. Chem. Soc. Faraday Trans. 2 **70**, 1552 (1974).

[52] T. Hollebeek, T. -S. Ho, and H. Rabitz, J. Chem. Phys. **114**, 3940 (2001).

[53] W.H. Press, S. A. Teukolsky, W. T. Vetterling, and B. P. Flannery, *Numerical Recipes in Fortran*, **2**nd edition (Cambridge University Press, Cambridge, 1992), p. 51.

[54] T. Xie, D. Wang, J. M. Bowman, and D. E. Manolopoulos, J. Chem. Phys. **116**, 7461 (2002).

[55] P.L. Fast, M.L. Sanchez, and D. G. Truhlar, Chem. Phys. Lett. **306**, 407 (1999).

[56] P.L. Fast, J.C. Corchado, M. L. Sanchez, and D. G. Truhlar, J. Phys. Chem. A **103**, 5129 (1999).

[57] C. M. Tratz, P. L. Fast, and D. G. Truhlar, PhysChemCommun. **2**/Article 14, 1, 1999.

[58] P. L. Fast and D. G. Truhlar, J. Phys. Chem. A **104**, 6111 (2000).

[59] A. Persky and M. Broida, J. Chem. Phys. **81**, 4352 (1984).

[60] T. -S. Ho, T. Hollebeek, H. Rabitz, L. B. Harding, and G. C. Schatz, J. Chem. Phys. **105**, 10472 (1996); G. C. Schatz, A. Papaioannou, L. A. Pederson, L. B. Harding, T. Hollebeek, T. -S. Ho, and H. Rabitz, J. Chem. Phys. **107**, 2340 (1997).

[61] T. Hollebeek, T. -S. Ho, H. Rabitz, L. B. Harding, J. Chem. Phys. **114**, 3945 (2001).

[62] T. -S. Ho, T. Hollebeek, H. Rabitz, S. D. Chao, R. T. Skodje, A. S. Zyubin, and A. M. Mebel, J. Chem. Phys. **116**, 4124 (2002).

[63] T. -S. Ho and H. Rabitz, J. Chem. Phys. **113**, 3960 (2000).

Figure Captions:

1. Three views of the $^3A''$ surface in (r_{OH},r_{HCl}) space corresponding to (a) the bent saddle point (θ_{OHCl} =135.9°), (b) the exit channel van der Waals well (θ_{OHCl} = 68.6°), and (c) the entrance channel van der Waals well (θ_{OHCl} = 180°). The range of contours are –5.5 to 88.0 kcal/mol. Negative energy (with respect to the asymptotic O + HCl minimum) contours are separated by 1.0 kcal/mol and are shown as dashed lines. The positive energy contours (solid lines) are separated by 2.0 kcal/mol up to 30 kcal/mol and then by larger intervals.

2. The dependence of the $^3A''$ and $^3A'$ potential surfaces on θ_{OHCl}. The solid lines show the angular dependences at bond lengths frozen at the respective minimum energy saddle point values. The dashed line shows the angular dependence of the $^3A''$ surface at bond-lengths corresponding to the collinear saddle point on the $^3A'$ surface.

3. Comparison of the variation of the potential energy along the minimum energy paths (MEPs) for the present $^3A''$ surface and the S4 surface of Ref. 14. The barrier on the present surface is "thicker" and higher than that on the S4 surface.

4. Contours of the scaled $^3A''$ surface as a function of H atom coordinates (x, y) relative to the Cl-O center of mass, for Cl and O located along the X-axis separated by $4.2422a_0$, the value corresponding to the exit channel van der Waals well minimum. The energies of the contours are the same as in Fig. 1. (a) A global view showing the van der Waals minimum (negative contours are shown as dashed lines). (b) An expanded view of the van der Waals well region.

Fig. 1

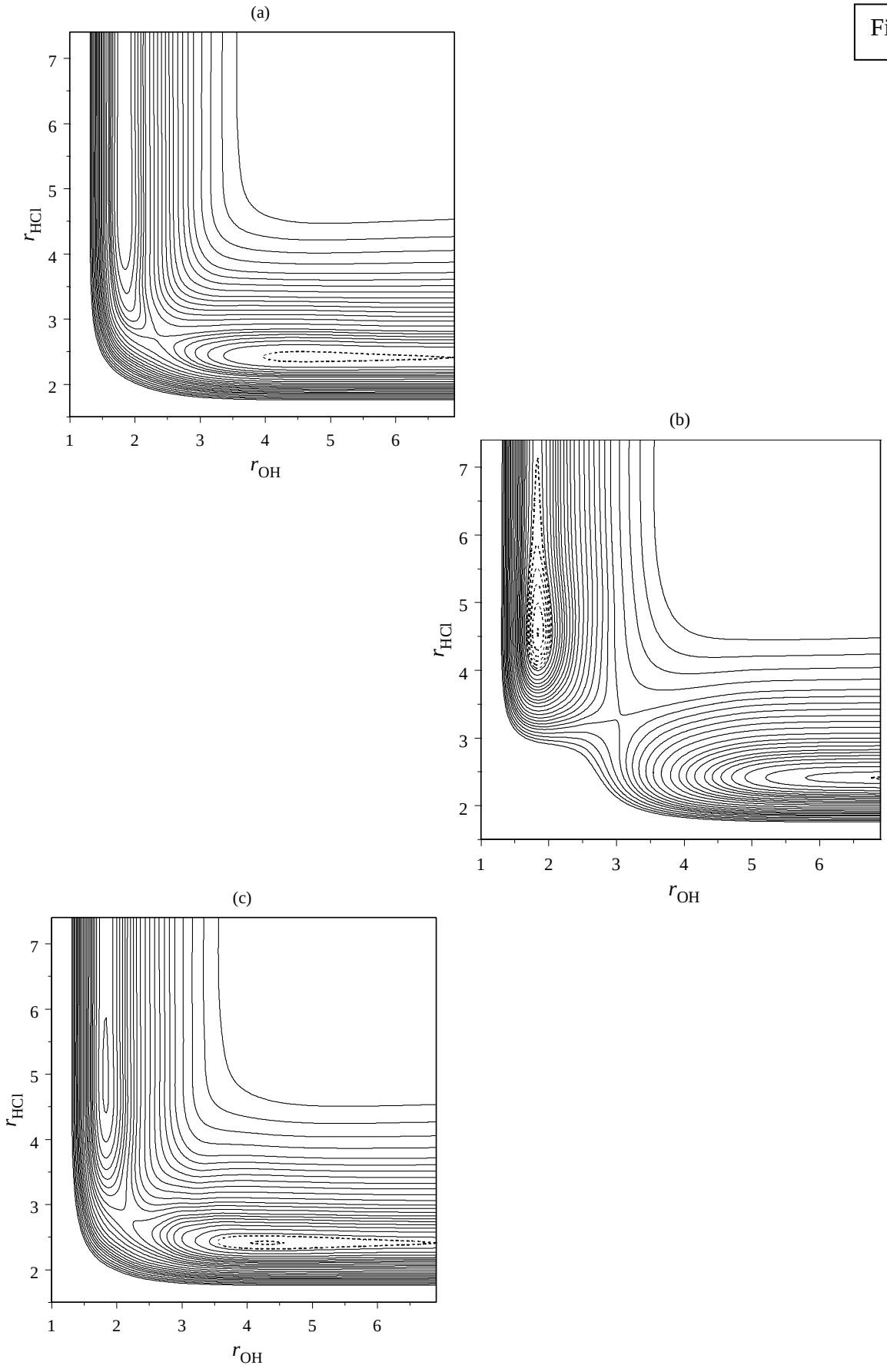

Fig. 2

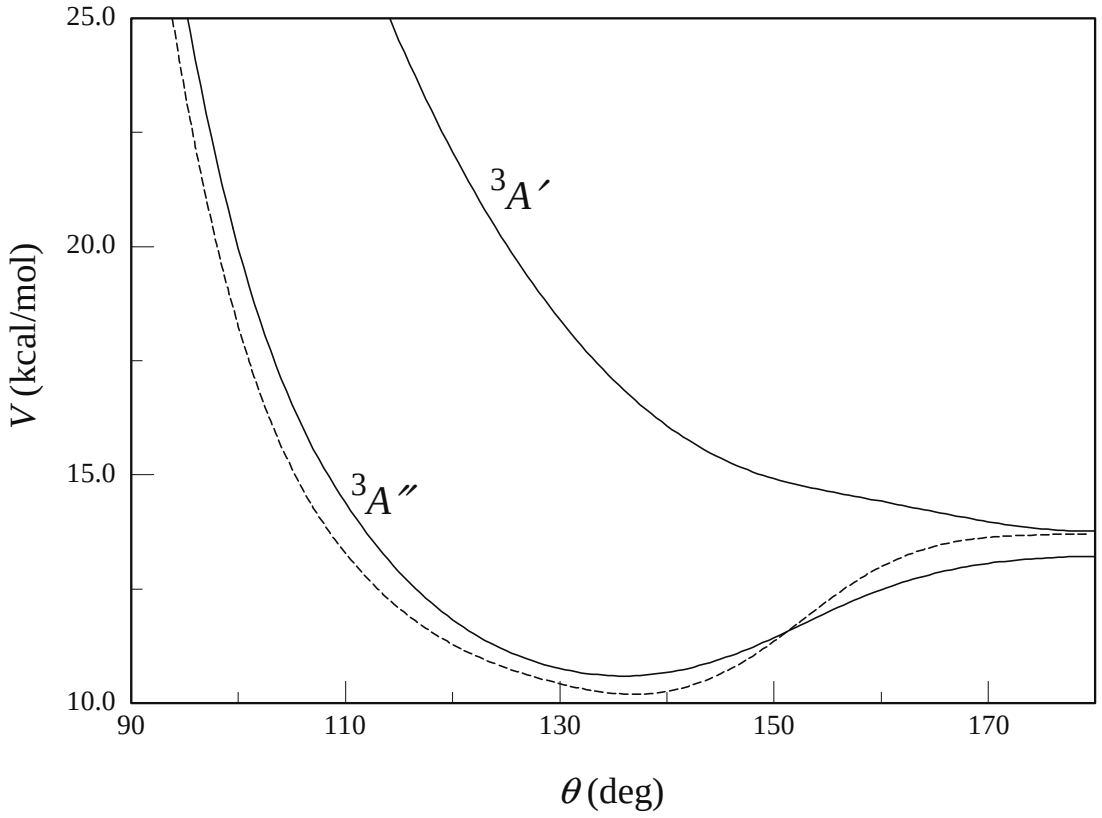
25.0
20.0
15.0
10.0
V (kcal/mol)
$^3A'$
$^3A''$
90
110
130
150
170
θ (deg)

Fig. 3

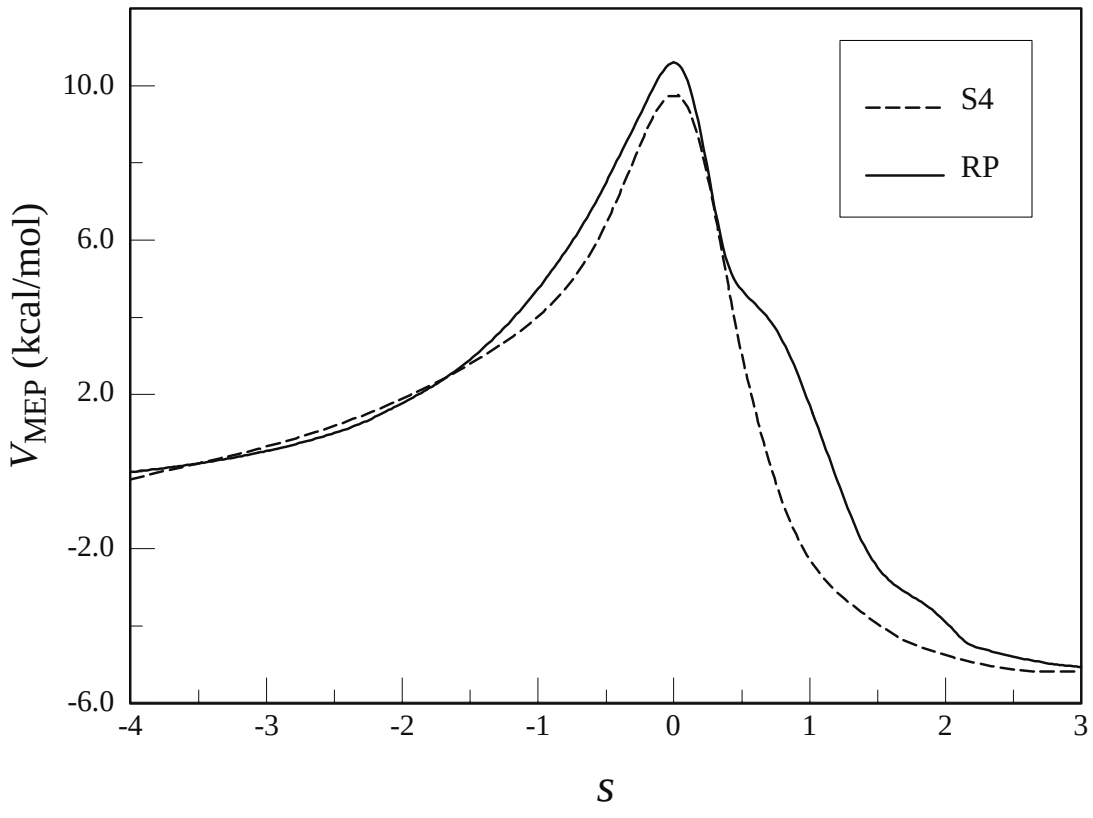
10.0
6.0
2.0
-2.0
-6.0
V_{MEP} (kcal/mol)
S4
RP
-4
-3
-2
-1
0
1
2
3
s

Fig. 4

(a)

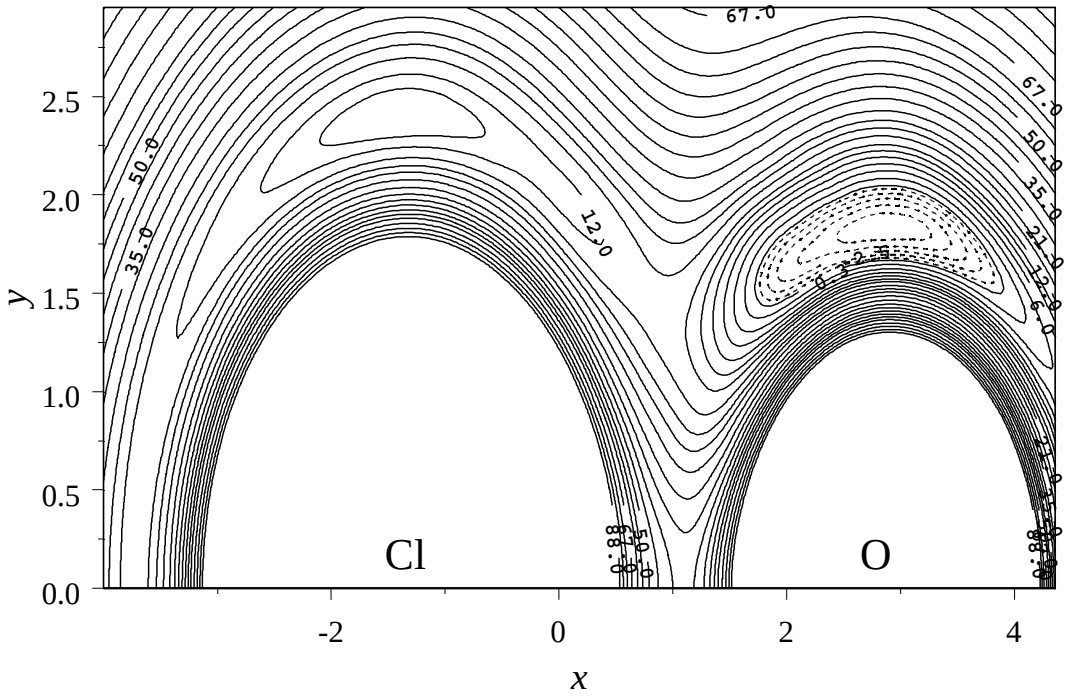
67.0
50.0
35.0
12.0
Cl
O
2.5
2.0
1.5
1.0
0.5
0.0
y
-2
0
2
4
x

(b)

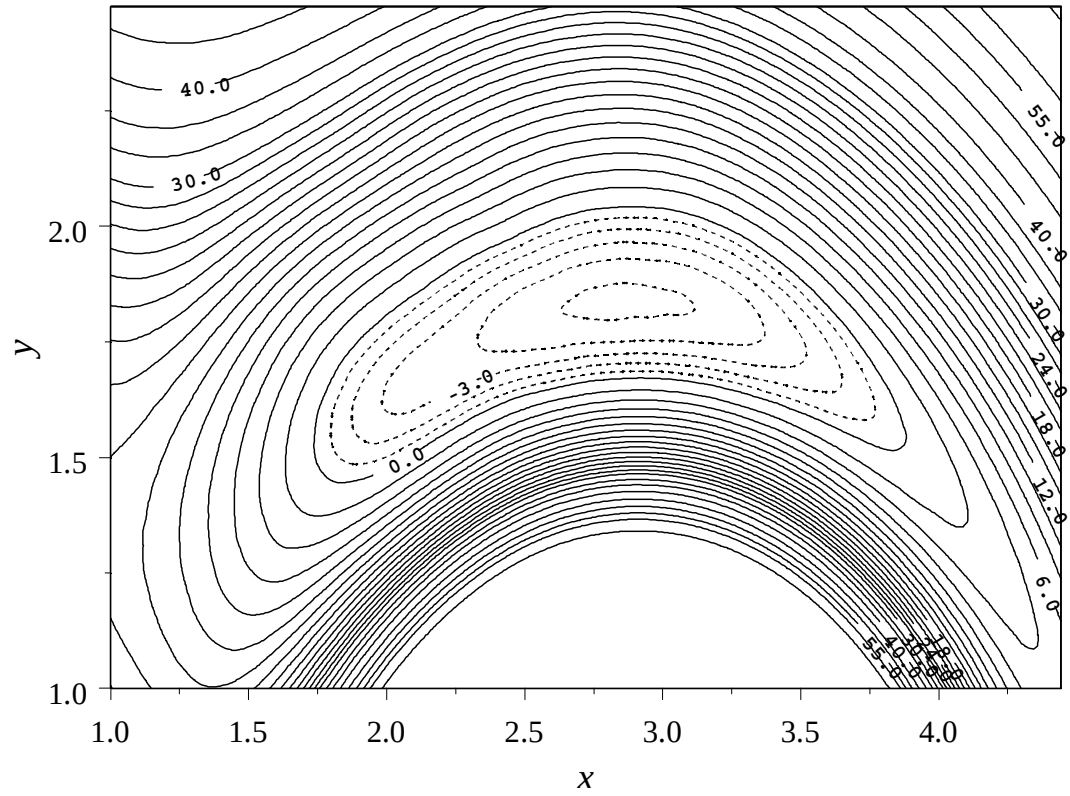
40.0
30.0
55.0
-3.0
0.0
24.0
18.0
12.0
6.0
2.0
1.5
1.0
y
1.0
1.5
2.0
2.5
3.0
3.5
4.0
x